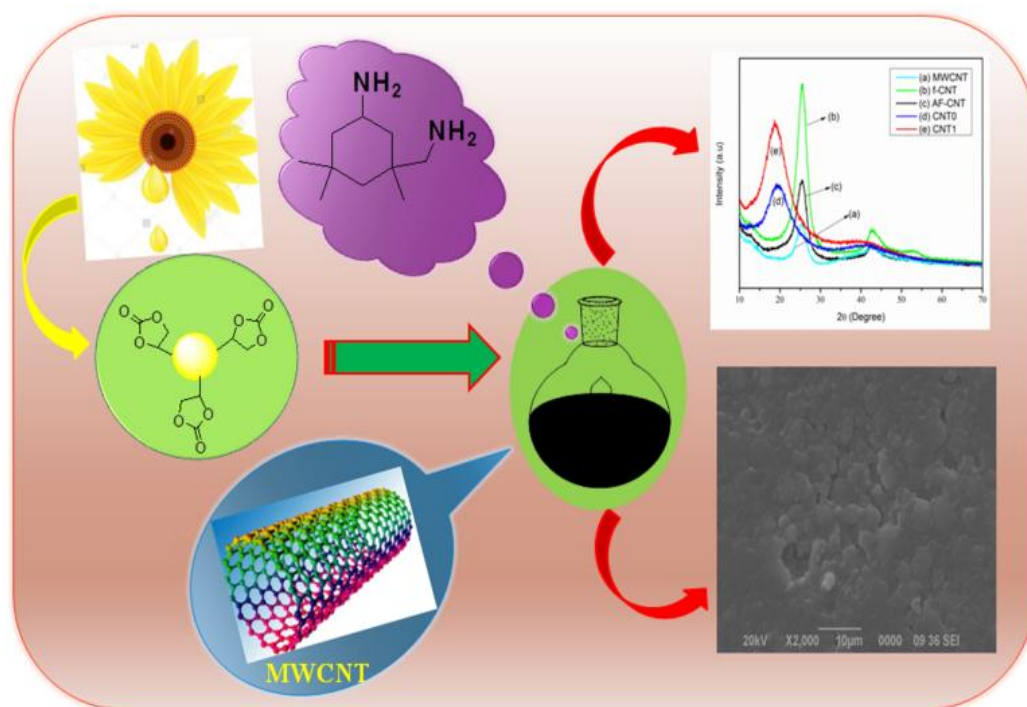# Chapter 4

Development of sunflower oil based non-isocyanate polyurethane/multi walled carbon nanotube composites with improved physico-chemical properties

This chapter describes the preparation of sunflower oil based non-isocyanate polyurethane and its nanocomposites with MWCNT with improved physico-chemical properties

Chapter 4: Development of sunflower oil based non-isocyanate polyurethane/multi walled carbon nanotube composites with improved physico-chemical properties

4.1 Introduction

CO_2 is known as one of the main greenhouse gases which is responsible for global warming and the major climate change in the 21st century [1]. Meanwhile, CO_2 is also an abundant, recyclable as well as inexpensive resource. So, from the standpoint of environmental safety, economic and resource consumption, the utilization of CO_2 as a renewable material for the preparation of valuable materials is highly advantageous [2–6]. An important utilization of CO_2 is in the preparation of five-membered cyclic carbonates *via* its reaction with epoxy substrates [2,3]. These cyclic carbonates have a large number of applications like aprotic polar solvents, electrolytes and precursor for polymer synthesis [7].

These cyclic carbonates are used as a precursor for the preparation of polyurethanes (the so-called non-isocyanate polyurethanes (NIPUs)) which avoid the use of isocyanates. Usually, conventional polyurethanes (PUs) are synthesized from isocyanates and polyols [8–10]. Isocyanates are highly toxic and volatile materials, and their long term exposure causes several harmful health effects [10]. The amount of methylene diphenyl diisocyanate (MDI) should be no more than 0.10 wt% in a constituent of mixtures [11]. Therefore, as concerns about health and safety, a substitute synthetic route needs to be developed for replacing isocyanates in the preparation of PUs from renewable resources.

The use of renewable resources in the production of polymers has attained global consideration by the reason of the environment safety and diminution of petroleum resources at high rate [12]. Amongst them, vegetable oils are attracting more

consideration owing to their easy availability and environmental friendly [12–14]. In addition, they can be chemically functionalized to give variety of products [15]. In recent time, various vegetable oils derived cyclic carbonates are being gradually used as precursor for synthesizing NIPUs [16–21]. NIPUs prepared by this way show better resistance to organic solvents and improved thermal stability [22,23,24]. However, due to steric hindrance of cyclic carbonated structures, the reactivity of amine or amide towards the cyclic carbonate is low [25].

In comparison to the conventional PUs, the low reactivity of secondary amine or amide towards the cyclic carbonates results in low molecular weight of NIPUs which affects its mechanical properties [26]. Therefore, to overcome these drawbacks of NIPUs, scientists are working on the development of catalysts and the design of molecular structures of cyclic carbonates up to seven-membered reactive cyclic carbonates to enhance the rate of the aminolysis reaction of the cyclic carbonates [27,28]. Researchers have found that 1,5,7-triazabicyclo[4.4.0]dec-5-ene is the most excellent catalyst to increase the reaction rate of aminolysis of cyclic carbonates [29]. However, this catalyst is very expensive.

To overcome these drawbacks, in this work amine functionalized multi walled carbon nanotube (AF-CNT) are incorporated into the polymer network of NIPU prepared by reacting carbonated sunflower oil (CSFO) with isophorone diamine (IPDA). (The prepared NIPU is also represented as CSFO/IPDA). Nanomaterials can play an key role in exceeding the limitations of conventional organic coatings and creating advanced coatings with longer lifetime [30]. Meanwhile, carbon nanotubes (CNT) have been considered broadly because of their exceptional electrical, thermal, mechanical properties, and high aspect ratios [31]. However, owing to inhomogeneous dispersion and interfacial bonding of the CNT, nanocomposites do not give the expected enhancement [32,33]. So, chemical functionalization at the surface is required to increase the polymer-CNT interaction by covalent interaction with pre-polymers and polymers [34]. In this work, we have used AF-CNT as the nano-filler and examined the influence of various wt% of AF-CNT in the properties of the NIPU.

4.2 Experimental

4.2.1 Materials

Multi walled carbon nanotube (MWCNT) was procured from Redex Technologies Pvt. Ltd., India. All the other chemicals used for the experiments are the same as mentioned in section 2.2.1 of Chapter 2.

4.2.2 Preparation of carbonated sunflower oil (CSFO)

Carbonated sunflower oil was prepared by reacting CO_2 with epoxidized sunflower oil (ESFO) at 120 °C and 40 bar CO_2 for 10 h catalyzed by tetra-n-butylammonium bromide (TBABr) (3.5 mol% with respect to the ESFO) in a reactor. After the desired time, the system was cooled down and the pressure was discharged to obtain the final product.

4.2.3 Amine modification of MWCNT (AF-CNT)

The pristine MWCNT (500 mg) was dispersed in HNO_3 (conc.) and ultra-sonicated for 2 h followed by refluxing and continuous stirring for 48 h at 85 ºC. After cooling down, the suspension was diluted by using 500 mL distilled water, filtered and subsequently washed with distilled water till neutral pH was attained. The resulting functionalized MWCNT (f-CNT) were kept at 60 ºC for 12 h in a vacuum oven.

f-CNT was silane functionalized according to the procedure reported by Zhu et al. [32]. The carboxylated MWCNT (f-CNT) were dispersed in toluene, and then (3-aminopropyl)trimethoxysilane (APTMS) (1 wt%) was subsequently added to the above solution. The resulting solution was refluxed at 110 ºC for 8 h. The resulting MWCNT (AF-CNT) were filtered and washed with distilled water and acetone. It was finally kept at 60 ºC for 24 h to evaporate water.

4.2.4 Preparation of NIPU and its nanocomposites with AF-CNT

The CSFO/IPDA/AF-CNT nanocomposites were synthesized by ring opening polymerization of CSFO by using IPDA as the curing agent. In a typical synthesis, AF-CNT (different wt%: 0.50, 1.0, 1.5 and 2 wt% with reference to CSFO) were dispersed in tetrahydrofuran (THF) and sonicated for 1 h to obtain uniform suspension of AF-

CNT. After obtaining stable dispersion of AF-CNT in THF, it was added to CSFO with continuous stirring for 3-4 h at 90 ºC with the addition of IPDA as the curing agent. A pristine NIPU sample (0 wt% AF-CNT) was also synthesized for comparison purpose and will be designated as CNT0. The resulting mixture was poured onto a Teflon sheet and heated at 85-90 ºC for 48 h followed by heating in oven at 110 ºC for 2 h to attain fully cured and freestanding NIPUs film. The constitutions of the nanocomposites with varying wt% of AF-CNT are given in **Table 4.1**.

Table 4.1: Composition of the nanocomposites.

Sample name	CSFO (g)	AF-CNT (wt%)	IPDA (g)
CNT0	5.0	0.0	1.54
CNT0.5	5.0	0.5	1.54
CNT1.0	5.0	1.0	1.54
CNT1.5	5.0	1.5	1.54
CNT2.0	5.0	2.0	1.54

CNT0 stands for NIPU without AF-CNT

* CNT0.5 stands for NIPU with 0.5 wt% AF-CNT and so on.*

4.2.5 Characterization

The instruments used for characterization including FT-IR, SEM, TGA and scratch hardness tester are discussed in section 2.2.4 of Chapter 2 and for XRD in section of 3.2.6 of Chapter 3. To examine the chemical resistance of the prepared films, small parts of the prepared polymer were kept in different concentration solutions.

4.3 Results and discussion

### 4.3.1 FT-IR studies:

4.3.1.1 Functionalization of MWCNT

FT-IR spectra of f-CNT and AF-CNT are presented in **Fig. 4.1**. In the FT-IR spectrum of f-CNT (**Fig. 4.1a**), peaks appear at 1738, 1069 and 889 cm^{-1} corresponding

to the carboxylic acid groups, C-O and the broad carboxylic acid -OH deformation respectively [35]. The peaks in the region of 2853-2928 cm^{-1} are observed in both the f-CNT and AF-CNT spectra due to C-H stretching. The results suggest that the successful introduction of carboxylic acid groups at the surface of the MWCNT. **Fig. 4.1b** presents the FT-IR spectrum of AF-CNT, the reaction product of f-CNT with APTMS. After silanization, two characteristic peaks are observed at 1581 and 695 cm^{-1} due to the primary amine of APTMS and weak N-H bending bonds [32]. The results show that COOH and silane moieties are effectively introduced at the surface of MWCNT by chemical treatment. The whole reaction process is represented diagrammatically in **Scheme 4.1**.
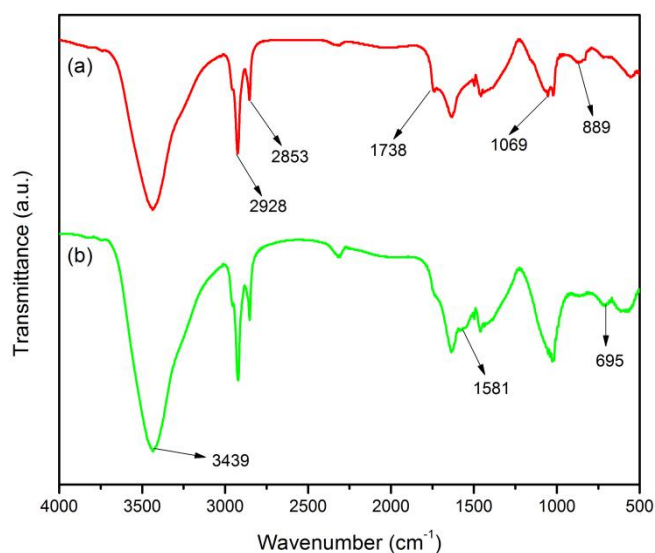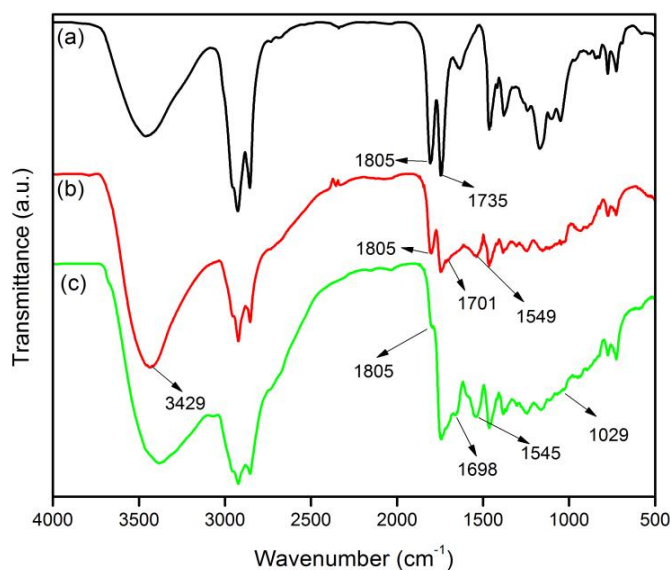

Fig. 4.1: FT-IR spectra of (a) f-CNT and (b) AF-CNT.
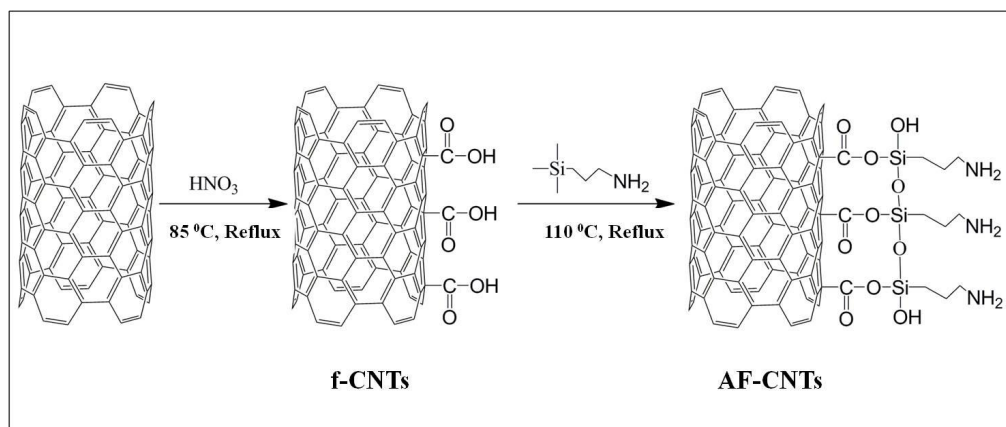
Scheme 4.1: Amine functionalization of MWCNT.

4.3.1.2 Preparation of NIPU and its nanocomposites with AF-CNT

**Fig. 4.2:** FT-IR spectra of (a) CSFO, (b) CNT0 and (c) CNT1.

FT-IR spectra of (a) CSFO, (b) CNT0 and (c) CNT1 are presented in **Fig. 4.2**. In the FT-IR spectrum of CSFO, the signal at 1805 cm^{-1} corresponds to carbonate stretching vibration (**Fig. 4.2a)**. In the case of CNT0 (**Fig. 4.2b)**, the presence of a shoulder peak at 1701 cm^{-1} indicates the formation of urethane along with a significant amount of residual cyclic carbonated at 1805 cm^{-1}. The broad peak at 3429 cm^{-1} is because of the hydroxyl groups resulting from the aminolysis of cyclic carbonated reaction and -NH stretching. In the FT-IR spectra of CNT1 (**Fig. 4.2c)**, signals at 1698, 1545 and1029 cm^{-1} represent the formation of urethane group, -NH deformation of urethane group and Si-O stretching of Si-O-C respectively. These peaks of NIPU along with AF-CNT confirm the formation of nanocomposites.

4.3.2 XRD analysis

XRD studies were carried out in order to examine whether there is a change in the structure of f-CNT and AF-CNT. The typical diffraction peak at 2θ = 25.7° for the plane (002) having interlayer distance 0.35 nm and another peak at 2θ = 43.18° for the plane (100) corresponding to the concentric cylinder structure of MWCNT are obtained in the XRD patterns of all the MWCNT (**Fig. 4.3.a, b, c**). Both acid functionalization and APTMS modification do not change the typical diffraction peaks of MWCNT, indicating

that chemical treatment of MWCNT does not destroy their structure. After the functionalization of the raw MWCNT, the intensity of the diffraction peak for the (002) plane is altered, it can be attributed to the different absorption coefficients of the functional groups and an increase in the graphitization degree due to the conversion of amorphous carbon [34].
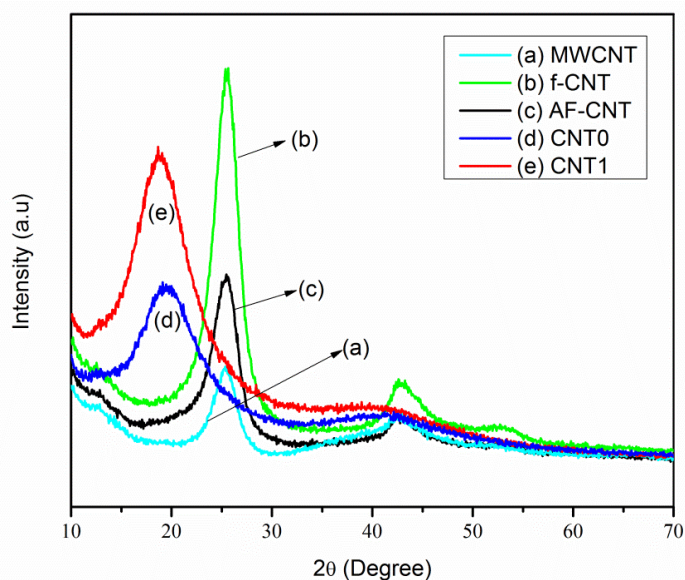
Fig. 4.3: XRD patterns of (a) MWCNT, (b) f-CNT, (c) AF-CNT (d) CNT0 and (e) CNT1.

XRD pattern of pristine CNT0 (**Fig. 4.3d**) shows a broad diffraction peak at around $2\theta = 19.01°$ which indicates some crystallinity of the pristine NIPU. Additionally, XRD pattern of the nanocomposite (CNT1) shows that the characteristic peak becomes sharp with the incorporation of AF-CNT (**Fig. 4.3e**). Noticeably, no typical diffraction peak belonging to the regular and periodic structure of the AF-CNT is observed in the nanocomposites. Thus, XRD pattern of the nanocomposite confirms the formation of fully exfoliated structure and the homogeneous distribution of AF-CNT within the NIPU [15].

4.3.3 SEM analysis

The surface of the CNT0 resin is represented in **Fig. 4.4a** which exhibited smooth surface. The surface of the nanocomposite CNT1 (**Fig. 4.4b)** shows a considerable increase in the surface roughness, which suggests the reinforcement of AF-CNT in

NIPU. The modification of the MWCNT enhanced their dispersion and interfacial bonding with the NIPU matrix because of the formation of reactive amine functional groups on their surfaces.
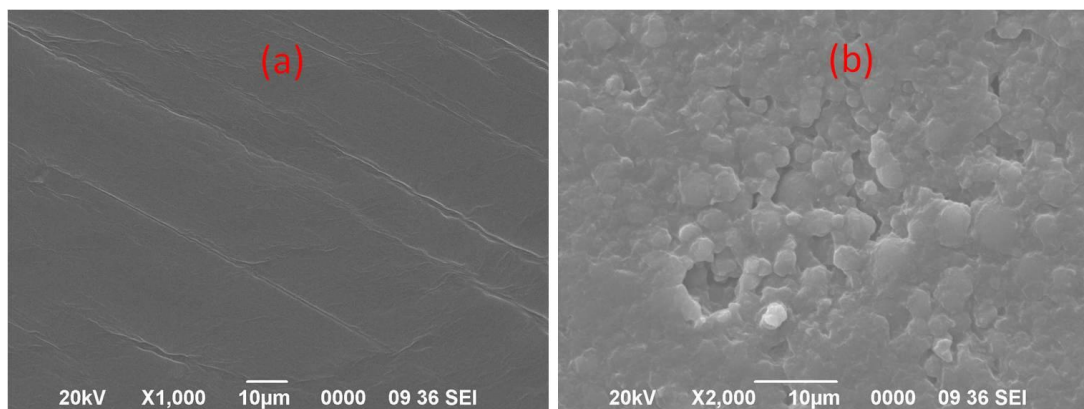

Fig. 4.4: SEM micrographs of (a) CNT0 and (b) CNT1 nanocomposite films.

4.3.4 Mechanical properties

The mechanical properties of the nanocomposites were observed by varying the wt% of AF-CNT content. From **Table 4.2**, it is seen that the tensile strength, scratch hardness and impact strength improves with the incorporation of AF-CNT. It can be attributed to the chemical bonding between the carbonate groups of CSFO and IPDA, and the amine groups on the surface of AF-CNT **(Scheme 4.2)**. Furthermore, hydrogen bonding between urethane, ester and hydroxyl groups also helps strong interfacial adhesion. The mechanical properties of the nanocomposites show a marked enhancement when 1.5 wt% of AF-CNT are added. The tensile strength of the pristine polymer network (CNT0) is initially 4.66 MPa which increases to 8.92 MPa with the incorporation of 1.5 wt% AF-CNT. This results compares favorably to other NIPUs based on soybean oil reported by Javni et al. [17]. At high loading of AF-CNT (2 wt%), these properties of the nanocomposites are decreased. This may be due to the fact that at high AF-CNT content, particle aggregation takes place. This improvement is attributed to the reinforcing effect of the CNT and uniformly dispersed AF-CNT in the CSFO/IPDA polymer network which hinders the motion of the polymer chains [15]. As a result of the reduced movement, a decrease in elongation at break of the nanocomposites is observed.
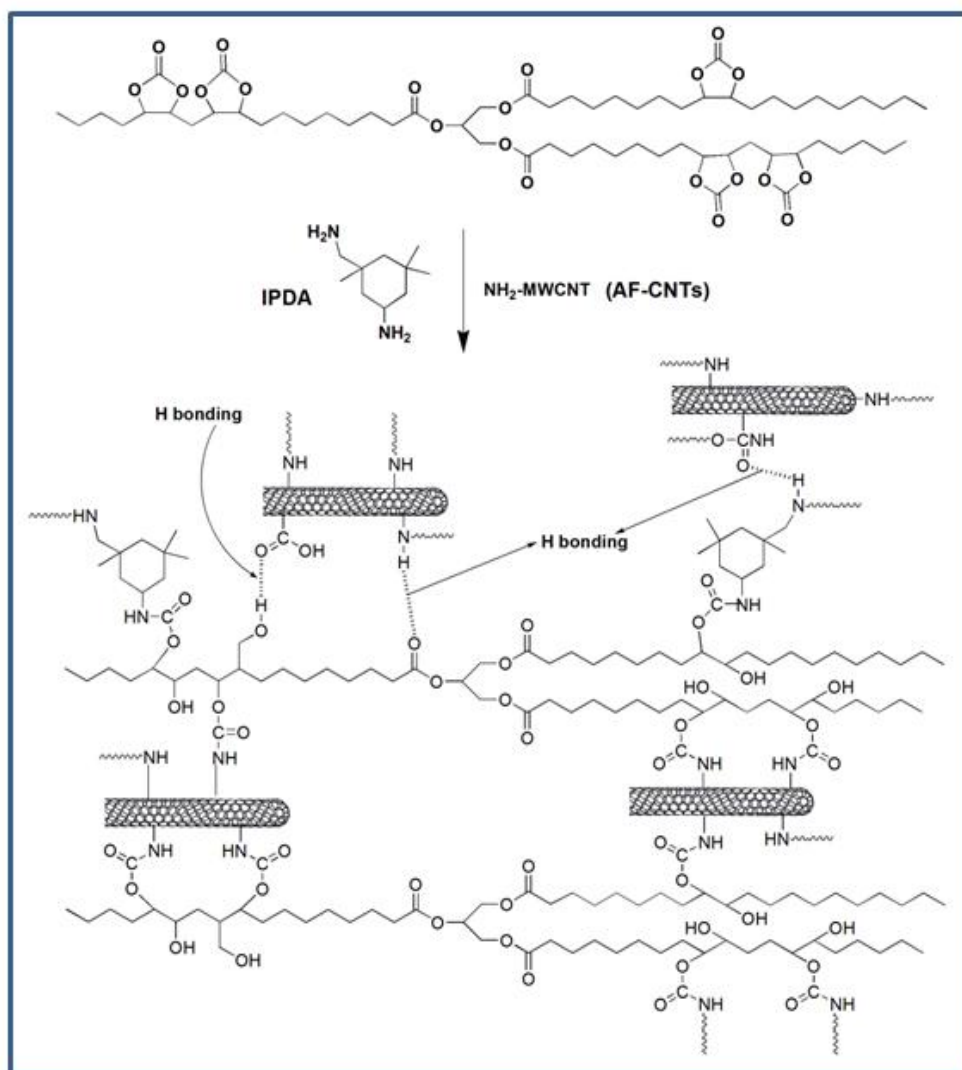
Scheme 4.2: Plausible cross-linked structure of the CSFO/IPDA/AF-CNT nanocomposites.
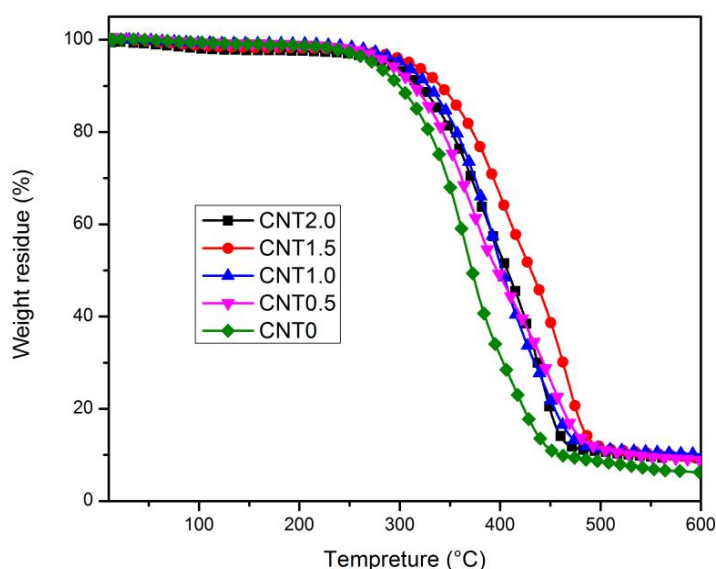
Table 4.2: Mechanical properties of the nanocomposites.

Sample name	Tensile strength (MPa)	Elongation at break (%)	Impact strength height (cm)	Scratch hardness (kg)
CNT0	4.66	290	63	3.5
CNT0.5	5.2	205	75	4.1
CNT1	7.20	171	86	4.8
CNT1.5	8.92	89	100	5.3
CNT2	4.92	273	77	4

4.3.5 Thermal stability

TGA thermograms of the nanocomposites are shown in **Fig. 4.5** and results are displayed in **Table 4.3**. From **Table 4.3**, it is suggested that nanocomposites have better thermal stability than CNT0. For example, a 5% weight loss of CNT0 takes place at 274 °C, whereas the same for the nanocomposite with 1 wt% of AF-CNT is increased by 28 °C. It is ascribed to the nano-mechanical interlocking of AF-CNT with the polymer matrix *via* the polar functionalities that can make possible electrostatic interactions and hydrogen bonding. Thermal stability is increased up to 1.5 wt% of AF-CNT and these properties decrease at 2 wt% of AF-CNT for CNT2. This is due to the steric hindrance

Fig. 4.5: TGA curves of the nanocomposites with different wt% of AF-CNT.

Table 4.3: Thermal properties of the nanocomposites.

Sample name	Temp @ 5% wt loss (°C	Temp @ 25% wt loss (°C)	Temp @ 50% wt loss (°C)
CNT0	274	347	390
CNT0.5	287	352	397
CNT1.0	302	366	401
CNT1.5	310	383	430
CNT2.0	289	353	393

and particle aggregation takes place at high AF-CNT loading. Due to the chemical bonding between the CSFO/IPDA and amine groups on the surface of the MWCNT, the mobility of polymer chains are reduced, thus slowing down its degradation [15]. These thermal properties are superior to those previously reported by Samanta et al. [18].

4.3.6 Chemical resistance analysis

The chemical resistance of the nanocomposites towards water, NaOH (5%, aq.), ethanol (25% aq.) and HCl (10% aq.) were tested for 20 days and the outcome are listed in **Table 4.4**. The prepared films posses high cross-linking density and rigid structure, so they exhibit excellent resistance to water, ethanol and HCl. But due to the presence of hydrolyzable ester linkages in pristine NIPU, the alkali resistance is only fair. Nonetheless, due to the formation of nanocomposites and cyclic-aliphatic structure of IPDA, the solvent diffusion is prohibited and the nanocomposites reveal suitable resistance to alkali.

Table 4.4: Chemical resistance tests for the nanocomposite films.

Sample name	Chemical Environment			
	Water	ethanol (25%, aq.)	NaOH (5%, aq.)	HCl (10%, aq.)
CNT0	Good	Excellent	Fair	Excellent
CNT0.5	Excellent	Excellent	Fair	Excellent
CNT1	Excellent	Excellent	Good	Excellent
CNT1.5	Excellent	Excellent	Good	Excellent
CNT2	Excellent	Excellent	Good	Excellent

*Excellent= No weight loss

4.4 Conclusion

Herein, we have developed an environmentally friendly NIPU/AF-CNT nanocomposite coating through an *in situ* catalyst-free, non-isocyanate method. Amine functionalization of MWCNT was done using an aqueous APTMS solution which is used as the nano-filler. As a result, the properties of composites increased in contrast to

pristine NIPUs. Furthermore, we observed that different wt% of the amine functionalized MWCNT (i.e., AF-CNT) had a significant impact on the chain confinement in the polymer network. The physico-chemical properties of the pristine NIPUs are enhanced considerably upon addition of AF-CNT. The nanocomposites were thermally stable and exhibited a tensile strength of 8.92 MPa with 89% elongation at break. It has been found that the properties of composites increase with the increase of AF-CNT content in the composites upto 1.5 wt%. The overall study suggests that the prepared nanocomposites are sustainable materials for coating applications.

4.5 References

[1]   Xu, S., Li, C., Li, H., Li, M., Qu, C., and Yang, B. Carbon dioxide sensors based on a surface acoustic wave device with a graphene-nickel-l -alanine multilayer film. *Journal of Materials Chemistry C*, 3(16):3882-3890, 2015.

[2]   Decortes, A., Castilla, A. M., and Kleij, A. W. Salen-complex-mediated formation of cyclic carbonates by cycloaddition of CO_2 to epoxides. *Angewandte Chemie International Edition*, 49(51):9822-9837, 2010.

[3]   North, M., Pasquale, R., and Young, C. Synthesis of cyclic carbonates from epoxides and CO_2. *Green Chemistry*, 12(9):1514, 2010.

[4]   Izumi, Y. Recent advances in the photocatalytic conversion of carbon dioxide to fuels with water and/or hydrogen using solar energy and beyond. *Coordination Chemistry Reviews*, 257(1):171-186, 2013.

[5]   Li, K., An, X., Park, K. H., Khraisheh, M., and Tang, J. A critical review of CO_2 photoconversion: Catalysts and reactors. *Catalysis Today*, 224:3-12, 2014.

[6]   Yang, Z. Z., He, L. N., Gao, J., Liu, A. H., and Yu, B. Carbon dioxide utilization with C-N bond formation: Carbon dioxide capture and subsequent conversion. *Energy & Environmental Science*, 5(5):6602, 2012.

[7]   Webster, D. C. Cyclic carbonate functional polymers and their applications. *Progress in Organic Coatings*, 47(1):77-86, 2003.

[8]   Bayer, O. The di-isocyanate -polyaddition (polyurethanes). *Angewandte Chemie International Edition*, 59(9):257-272, 1947.

[9]   Chen, S., Yuan, H., Ge, Z., Chen, S., Zhuo, H., and Liu, J. Insights into liquid-crystalline shape-memory polyurethane composites based on an amorphous reversible phase and hexadecyloxybenzoic acid. *Journal of Materials Chemistry C*, 2(6):1041-1049, 2014.

[10]   Maisonneuve, L., Lamarzelle, O., Rix, E., Grau, E., and Cramail, H. Isocyanate-free routes to polyurethanes and poly(hydroxy urethane)s. *Chemical Reviews*, 115(22):12407-12439, 2015.

[11]   Nohra, B., Candy, L., Blanco, J. F., Guerin, C., Raoul, Y., and Mouloungui, Z. From petrochemical polyurethanes to biobased polyhydroxyurethanes. *Macromolecules*, 46(10):3771-3792, 2013.

[12]   Gogoi, P., Boruah, M., Sharma, S., and Dolui, S. K. Blends of epoxidized alkyd

resins based on jatropha oil and the epoxidized oil cured with aqueous citric acid solution: A Green technology approach. *ACS Sustainable Chemistry & Engineering*, 3(2):261-268, 2015.

[13] Yu, J., Du, Y., Zheng, H., and Cheng, F. Properties and interfacial bonding for regenerated cellulose-polyurethane/amylose acetate sipn composite films. *Polymer Composites*, 21(6):872-877, 2000.

[14] Kuncho, C. N., Schmidt, D. F., and Reynaud, E. Effects of catalyst content, anhydride blending, and nanofiller addition on anhydride-cured epoxidized linseed oil-based thermosets. *Industrial & Engineering Chemistry Research*, 56(10):2658-2666, 2017.

[15] Gogoi, P., Boruah, R., and Dolui, S. K. Jatropha curcas oil based alkyd/epoxy/graphene oxide (GO) bionanocomposites: Effect of GO on curing, mechanical and thermal properties. *Progress in Organic Coatings*, 84:128-135, 2015.

[16] Bähr, M. and Mülhaupt, R. Linseed and soybean oil-based polyurethanes prepared via the non-isocyanate route and catalytic carbon dioxide conversion. *Green Chemistry*, 14(2):483, 2012.

[17] Javni, I., Hong, D. P., and Petrović, Z. S. Soy-based polyurethanes by nonisocyanate route. *Journal of Applied Polymer Science*, 108(6):3867-3875, 2008.

[18] Samanta, S., Selvakumar, S., Bahr, J., Wickramaratne, D. S., Sibi, M., and Chisholm, B. J. Synthesis and characterization of polyurethane networks derived from soybean-oil-based cyclic carbonates and bioderivable diamines. *ACS Sustainable Chemistry & Engineering*, 4(12):6551-6561, 2016.

[19] Rokicki, G. and Piotrowska, A. A new route to polyurethanes from ethylene carbonate, diamines and diols. *Polymer*, 43(10):2927-2935, 2002.

[20] Ochiai, B., Inoue, S., and Endo, T. One-pot non-isocyanate synthesis of polyurethanes from bisepoxide, carbon dioxide, and diamine. *Journal of Polymer Science Part A: Polymer Chemistry*, 43(24):6613-6618, 2005.

[21] Besse, V., Foyer, G., Auvergne, R., Caillol, S., and Boutevin, B. Access to nonisocyanate poly(thio)urethanes: A comparative study. *Journal of Polymer Science Part A: Polymer Chemistry*, 51(15):3284-3296, 2013.

[22] Tomita, H., Sanda, F., and Endo, T. Reactivity comparison of five- and six-membered cyclic carbonates with amines: Basic evaluation for synthesis of poly(hydroxyurethane). *Journal of Polymer Science Part A: Polymer Chemistry*, 39(1):162-168, 2001.

[23] Bähr, M., Bitto, A., and Mülhaupt, R. Cyclic limonene dicarbonate as a new monomer for non-isocyanate oligo- and polyurethanes (NIPU) based upon terpenes. *Green Chemistry*, 14(5):1447, 2012.

[24] Rokicki, G., Parzuchowski, P. G., and Mazurek, M. Non-isocyanate polyurethanes: Synthesis, properties, and applications. *Polymers for Advanced Technologies*, 26(7):707-761, 2015.

[25] Besse, V., Camara, F., Méchin, F., Fleury, E., Caillol, S., Pascault, J. P., and Boutevin, B. How to explain low molar masses in polyhydroxyurethanes (PHUs). *European Polymer Journal*, 71:1-11, 2015.

[26] Ke, J., Li, X., Wang, F., Kang, M., Feng, Y., Zhao, Y., and Wang, J. The hybrid polyhydroxyurethane materials synthesized by a prepolymerization method from CO_2-sourced monomer and epoxy. *Journal of CO_2 Utilization*, 16:474-485, 2016.

[27] Maisonneuve, L., Wirotius, A. L., Alfos, C., Grau, E., and Cramail, H. Fatty acid-based (bis) 6-membered cyclic carbonates as efficient isocyanate free poly(hydroxyurethane) precursors. *Polyemer Chemistry*, 5(21):6142-6147, 2014.

[28] Tomita, H., Sanda, F., and Endo, T. Polyaddition behavior of bis(five- and six-membered cyclic carbonate)s with diamine. *Journal of Polymer Science Part A: Polymer Chemistry*, 39(6):860-867, 2001.

[29] Tang, D., Mulder, D. J., Noordover, B. A. J., and Koning, C. E. Well-defined biobased segmented polyureas synthesis via a TBD-catalyzed isocyanate-free route. *Macromolecular Rapid Communications*, 32(17):1379-1385, 2011.

[30] Vennerberg, D., Rueger, Z., and Kessler, M. R. Effect of silane structure on the properties of silanized multiwalled carbon nanotube-epoxy nanocomposites. *Polymer*, 55(7):1854-1865, 2014.

[31] Zhang, C., Vennerberg, D., and Kessler, M. R. *in situ* synthesis of biopolyurethane nanocomposites reinforced with modified multiwalled carbon nanotubes. *Journal of Applied Polymer Science*, 132(36):42515, 2015.

[32] Zhu, J., Wei, S., Yadav, A., and Guo, Z. Rheological behaviors and electrical

conductivity of epoxy resin nanocomposites suspended with in-situ stabilized carbon nanofibers. *Polymer*, 51(12):2643-2651, 2010.

[33] Wagner, H. D. and Vaia, R. A. Nanocomposites: Issues at the interface. *Materials Today*, 7(11):38-42, 2004.

[34] Sankal, S. and Kaynak, C. Using various techniques to characterize oxidative functionalized and aminosilanized carbon nanotubes for polyamide matrix. *Journal of Reinforced Plastics and Composites*, 32(2):75-86, 2013.

[35] Bora, A., Mohan, K., Pegu, D., Gohain, C. B., and Dolui, S. K. A room temperature methanol vapor sensor based on highly conducting carboxylated multi-walled carbon nanotube/polyaniline nanotube composite. *Sensors and Actuators B: Chemical*, 253:977-986, 2017.